Decoupled Beamforming and Power Allocation in Integrated Sensing and Communication for WLAN

Hasan Can Yildirim, *Member, IEEE*, Laurent Storrer, *Member, IEEE*, Martin Willame, *Member, IEEE*, Jerome Louveaux, *Fellow, IEEE*, François Horlin, *Fellow, IEEE*

***Abstract*—This paper presents a novel framework for integrated sensing and communication in WLAN systems. The proposed approach adapts multi-user multi-input multi-output precoder of Wi-Fi systems to enable simultaneous communication and sensing and simplifies power allocation between both tasks as an independent optimization problem while requiring minimal software upgrades. A flexible power allocation method optimizes signal-to-noise-plus-interference-ratio (SINR) balancing for users and targets, accommodating trade-offs between communication and sensing. Numerical results demonstrate the framework's effectiveness in achieving balanced SINR and enhancing integrated sensing and communication (ISAC) performance.**

***Index Terms*—ISAC, JCAS, WLAN sensing, power allocation, SINR balancing**

I. Introduction

The Wi-Fi standard is evolving by periodically introducing new amendments. The 802.11ac amendment brought multi-user multiple-input multiple-output (MU-MIMO) technology to deal with dense deployment scenarios, enabling access points (APs) to form directive radio waves toward multiple users. This process begins with the AP initiating a channel-sounding session by transmitting predefined Wi-Fi frames called *null data packets* (NDPs) [1]. User devices estimate their channel coefficients from the received NDPs on a *per-subcarrier basis* and send this information back to the AP. Using this explicit feedback, the AP computes a zero-forcing precoder (ZFP) to enable MU-MIMO data transmission, where *only the data fields are precoded, but not the preamble*.

Recently, the 802.11bf amendment introduced WLAN sensing [2], expanding the Wi-Fi framework to support sensing applications [3]. This feature repurposes the channel-sounding mechanism and NDPs for radar-like sensing tasks, utilizing channel coefficients to generate range/Doppler/angle maps. However, the current *Wi-Fi* implementation has two key limitations: i) it *does not leverage the precoding capabilities of APs*, meaning NDPs are not precoded, and ii) it *does not support simultaneous communication and sensing*.

Meanwhile, wireless communication and radar technologies are converging under a unified framework: integrated sensing and communication (ISAC) [4]. There are two approaches to developing ISAC systems. The *co-existence* approach ensures that sensing and communication subsystems operate by sharing the resources (time, frequency, and space), and therefore necessitate resource allocation and interference mitigation [5], [6]. However, the subsystems are designed independently and adjusted to coexist harmoniously. In contrast, the *co-design* approach jointly develops sensing and communication subsystems from the outset by generating an optimized signal that can serve both functionalities [7]. This method accounts for the requirements and constraints of both systems during the design process especially since communication requires random channels and signals, while sensing requires deterministic ones [8]. Examples of ISAC enhancements achieved through co-design include dual-functional waveform optimization [9], adaptive transmit beamforming [10], and adaptive power allocation [11], all of which balance radar accuracy with communication quality. In addition to these approaches, the fundamental performance bounds of ISAC systems have been analyzed using an information-theoretic framework [12], [13]. Additionally, a comprehensive survey on ISAC waveform design is provided in [14], offering valuable insights into the development of these integrated systems.

The 802.11bf amendment, independently developed from the communication-centric aspects of the Wi-Fi standard, positions Wi-Fi closer to the co-existence model than the co-design paradigm. In our previous works, we investigated the MU-MIMO precoding of the preambles used for sensing in a co-existence approach. We first studied how the precoder impacts the sensing coverage in a passive radar context where the data fields are also used for sensing [15]. We then demonstrated that the knowledge of the precoder at the sensing device enables the estimation of the AoD from the transmitter [16]. Recently, we showed that the zero-forcing precoder (ZFP) can significantly improve WLAN sensing accuracy when it is used to precode the preambles as well [17].

In this paper, we are moving to the co-design approach where a single signal is transmitted to support simultaneous communication and sensing. We propose a novel approach to enhance WLAN with ISAC. Unlike prior studies that jointly optimize beamforming weights and power allocation under specific constraints, our method builds upon [18] by leveraging the existing ZFP to enable simultaneous communication and sensing, while treating power allocation as an independent optimization problem. As a result, *the proposed method is achievable with relatively straightforward software upgrades in the WLAN standard*. Our contributions are listed as follows:

- **A novel ISAC framework for WLAN:** We propose an ISAC enhancement by using ZFP for *simultaneous communication and sensing*. This simplifies the implementation by separating beamforming and power allocation, making it practical in WLAN systems.

H. C. Yildirim, L. Storrer, and F. Horlin are with Université Libre de Bruxelles, while M. Willame and J. Louveaux are with Université Catholique de Louvain.

- **Flexible power allocation:** We develop a gradient-descent-based power allocation optimization framework to balance signal-to-interference-plus-noise-ratio (SINR) between users and targets on a per subcarrier basis. The framework is flexible enough to support SINR balancing among users and targets, or subsystem prioritization while ensuring compliance with power constraints.
- **Performance evaluation:** Numerical results demonstrate the balanced SINR performance for simultaneous communication and sensing under diverse configurations.

Notation: Bold letters represent vectors $\mathbf{v}$ and matrices $\mathbf{M}$, while $\|\mathbf{v}\|^2$ and $\|\mathbf{M}\|^2$ represent the Euclidean and Frobenius norms. The kth column of $\mathbf{M}$ is $\mathbf{m}_k$, and the averaging vector is $\mathbf{1}_N = [\frac{1}{N} \dots \frac{1}{N}]^T \in \mathbb{R}^{N\times 1}$.

II. Simultaneous Communication and Sensing

To enable simultaneous communication and sensing in WLAN, we propose extending ZFP to precode both the data symbols for communication and the training fields for sensing, and transmit a signal that serves both purposes. Under the narrowband assumption, the simplified transmit signal per subcarrier is defined as

$$\begin{aligned}\mathbf{s} &= \underbrace{\mathbf{W}\mathbf{\Lambda}_\gamma\mathbf{c}}_{\text{Communication}} + \underbrace{\mathbf{D}\mathbf{\Lambda}_\eta\mathbf{x}}_{\text{Sensing}} \\ &= \sum_{u=1}^{U}\mathbf{w}_u\gamma_u c_u + \sum_{k=1}^{K}\mathbf{d}_k\eta_k x_k, \in \mathbb{C}^{N_T\times 1} \qquad (1)\end{aligned}$$

where N_T is the number of transmit antennas, $\mathbf{W} \in \mathbb{C}^{N_T\times U}$ and $\mathbf{D} \in \mathbb{C}^{N_T\times K}$ are the precoders used for transmitting data to U number of users and sensing signals to K number of targets, respectively. The ISAC system is feasible for $U + K \leq N_T$. Meanwhile, $\mathbf{\Lambda}_\gamma \in \mathbb{R}^{U\times U}$ and $\mathbf{\Lambda}_\eta \in \mathbb{R}^{K\times K}$ are diagonal matrices whose entries are defined as $\sqrt{\gamma_u}$ and $\sqrt{\eta_k}$ corresponding to *the power allocated for user* u and *target* k, respectively, satisfying the constraint $\sum_u \gamma_u + \sum_k \eta_k \leq P_T$ where P_T is the total transmit power. The data symbols per user and the training symbols for sensing are given in $\mathbf{c} \in \mathbb{C}^{U\times 1}$ and $\mathbf{x} \in \mathbb{C}^{K\times 1}$, respectively.

A. Zero-Forcing Precoder in Wi-Fi

Let θ_u and ϕ_k represent the angles of departure (AoD) for the users and the targets[1], respectively, and the transmit steering vector is defined as $\mathbf{a}_T(\psi) = [1\ e^{j\pi\sin(\psi)}\ \dots\ e^{j(N_T-1)\pi\sin(\psi)}]^T \in \mathbb{C}^{N_T\times 1}$ where the antenna spacing is assumed to be half of the carrier wavelength. Then, the steering matrices for users and targets are given as $\mathbf{\Theta} = [\mathbf{a}_T(\theta_1)\dots\mathbf{a}_T(\theta_K)] \in \mathbb{C}^{N_T\times U}$ and $\mathbf{\Phi} = [\mathbf{a}_T(\phi_1)\dots\mathbf{a}_T(\phi_K)] \in \mathbb{C}^{N_T\times K}$, respectively. By combining all the angles, $\mathbf{\Psi} = [\mathbf{\Theta}\ \mathbf{\Phi}] \in \mathbb{C}^{N_T\times U+K}$, the ISAC ZFP is obtained as

$$\mathbf{P}_0 = \mathbf{\Psi}(\mathbf{\Psi}^{\mathsf{H}}\mathbf{\Psi})^{-1} \in \mathbb{C}^{N_T\times U+K} \qquad (2)$$

where the columns of $\mathbf{\Psi}$, i.e., the steering vectors, can be obtained i) during a prior channel sounding with explicit feedback from users [1] and ii) at the end of a prior sensing session where the angles of targets-of-interest are detected [17][2]. The first U columns of $\mathbf{P}_0$ correspond to $\mathbf{W}$ while the remaining K columns are for $\mathbf{D}$. It is important to mention that while *ZFP theoretically eliminates interference, practical implementations experience residual interference* caused by factors such as antenna calibration errors, quantized channel feedback, finite sampling resolution, channel correlation, rank deficiency, and hardware impairments [19], [20].

B. Communication Perspective per User

1) Communication channel: The communication channel per user u on a given subcarrier is defined as $\mathbf{G}_u \in \mathbb{C}^{N_u\times N_T}$ where N_u is the number of receiver antennas. If LoS is present, the entries in $\mathbf{G}_u$ follow a Rician distribution, otherwise, a Rayleigh distribution. We refer to [21], [22] for more details.

2) Received Signal: The signal at user u is given as

$$\hat{\mathbf{y}}_u = \mathbf{G}_u\mathbf{s} + \mathbf{z}_u = \mathbf{G}_u\mathbf{W}\mathbf{\Lambda}_\gamma\mathbf{c} + \mathbf{G}_u\mathbf{D}\Lambda_\eta\mathbf{x} + \mathbf{z}_u, \in \mathbb{C}^{N_R\times 1}$$

where $\mathbf{G}_u\mathbf{W}\mathbf{\Lambda}_\gamma\mathbf{c}$ corresponds to the signal of interest, $\mathbf{G}_u\mathbf{D}\mathbf{\Lambda}_\eta\mathbf{x}$ is the interference from sensing signals, and $\mathbf{z}_u$ is the additive white Gaussian noise (AWGN).

3) SINR: The generic SINR for the uth user is given in compact form as

$$\Upsilon_u = \frac{\gamma_u\alpha_u}{\sigma_u^2 + \sum_{v\neq u}\gamma_v\alpha'_{u,v} + \sum_k \eta_k\alpha''_{u,k}} \qquad (3)$$

where the path gains, obtained upon applying the corresponding precoders, are defined as $\alpha_u = \|\mathbf{G}_u\mathbf{w}_u c_u\|^2$, $\alpha'_{u,v} = \|\mathbf{G}_u\mathbf{w}_v c_v\|^2$, and $\alpha''_{u,k} = \|\mathbf{G}_u\mathbf{d}_k x_k\|^2$. Here, $\mathbf{w}_u$ and $\mathbf{d}_k$ correspond to the uth column of $\mathbf{W}$ and the kth column of $\mathbf{D}$, respectively, and $u \neq v$. The terms in the denominator correspond to the noise variance at user u, the interference from other users, and the interference from the sensing subsystem, respectively.

C. Sensing Perspective per Target

1) Sensing Channel: We assume each target has a LoS to both the AP and the receiver (Rx). Hence, the sensing channel for the kth target per subcarrier is defined as

$$\mathbf{H}_k = A_k\mathbf{a}_R(\varphi_k)\mathbf{a}_T^{\mathsf{H}}(\phi_k) + \bar{\mathbf{H}}_k \in \mathbb{C}^{N_R\times N_T} \qquad (4)$$

where A_k is the complex gain incorporating the delay and Doppler information. The steering vector at Rx is defined as $\mathbf{a}_R(\varphi_k) = [1\ e^{\pi\sin(\varphi_k)}\ \dots\ e^{j(N_R-1)\pi\sin(\varphi_k)}]^T, \in \mathbb{C}^{N_R\times 1}$ where φ_k is the AoA of target k, and the antenna spacing is half of the carrier wavelength. Hence, the first term in (4) refers to the LoS, while the second term ($\bar{\mathbf{H}}_k$) corresponds to the diffuse scatterings and multipath components, typically following a Rayleigh distribution [22]. Then, the overall sensing channel is given as $\mathbf{H} = \sum_k \mathbf{H}_k \in \mathbb{C}^{N_R\times N_T}$.

2) Received Signal: The signal at sensing-Rx is given as

$$\hat{\mathbf{r}}_k = \mathbf{H}_k\mathbf{s} + \mathbf{z} = \mathbf{H}_k\mathbf{W}\mathbf{\Lambda}_\gamma\mathbf{c} + \mathbf{H}_k\mathbf{D}\mathbf{\Lambda}_\eta\mathbf{x} + \mathbf{z}, \in \mathbb{C}^{N_R\times 1}$$

where $\mathbf{H}_k\mathbf{W}\mathbf{\Lambda}_\gamma\mathbf{c}$ and $\mathbf{H}_k\mathbf{D}\mathbf{\Lambda}_\eta\mathbf{x}$ correspond to the signal-of-interest and the interference from communication subsystem, while $\mathbf{z}$ is the AWGN at sensing-Rx.

[1] The AoDs θ_u and ϕ_k are not necessarily the line-of-sight. They are simply a subset of the eigenmodes of the channel corresponding to the users and targets. We refer to [1] to describe the standardized MU-MIMO procedure in detail.

[2] In its current form, the WLAN standard uses only $\mathbf{\Phi} = \mathbf{\Theta}$ to construct the MU-MIMO ZFP.

3) SINR: The SINR per target k is given in compact form as follows

$$\Xi_k = \frac{\eta_k \beta_k}{\sigma_r^2 + \sum_u \gamma_u \beta''_{k,u} + \sum_{i \neq k} \eta_i \beta'_{k,i}} \tag{5}$$

where the path gains are defined as $\beta_k = \|\mathbf{H}_k \mathbf{d}_k x_k\|^2$, $\beta''_{k,u} = \|\mathbf{H}_k \mathbf{w}_u c_u\|^2$, and $\beta'_{k,i} = \|\mathbf{H}_k \mathbf{d}_i x_i\|^2$ where $k \neq i$. The terms in the denominator are the noise variance at the sensing receiver, the interference from the communication subsystem, and the interference from sensing, respectively.

III. Power Allocations based on SINR

In addition to ZFP, we aim to optimize power allocation across U users and K sensing targets while adhering to the following constraints: i) the total allocated power per subcarrier must not exceed the available transmit power per subcarrier P_T, and ii) each allocated power must be non-negative. Furthermore, depending on the priorities of the ISAC system, our proposed power allocation method can be customized i) to prioritize one subsystem over the other, and ii) to balance SINR within each subsystem, i.e., among users and targets, for a fair ISAC signal transmission.

A. Generic Objective Function

Let us first gather the user and target SINRs in vector form $\boldsymbol{\Upsilon} = [\Upsilon_1 \dots \Upsilon_U]^T \in \mathbb{R}^{U \times 1}$ and $\boldsymbol{\Xi} = [\Xi_1 \dots \Xi_K]^T \in \mathbb{R}^{K \times 1}$, as well as the allocated powers $\boldsymbol{\gamma} = [\gamma_1 \dots \gamma_U]^T \in \mathbb{R}^{U \times 1}$ and $\boldsymbol{\eta} = [\eta_1 \dots \eta_K] \in \mathbb{R}^{K \times 1}$. Then, we define the optimization problem as follows

$$\begin{aligned} &\underset{\gamma_u, \eta_k, \forall u,k}{\arg\min} \; f(\boldsymbol{\gamma}, \boldsymbol{\eta}) = \mathbf{1}_U^T \boldsymbol{\Upsilon}^{-1} + \lambda_s \mathbf{1}_K^T \boldsymbol{\Xi}^{-1} \\ &\text{s.t.} \sum_{u=1}^{U} \gamma_u + \sum_{k=1}^{K} \eta_k \leq P_T, \quad \gamma_u \geq 0, \forall u, \quad \eta_k \geq 0, \forall k. \end{aligned} \tag{6}$$

where $\boldsymbol{\Upsilon}^{-1}$ and $\boldsymbol{\Xi}^{-1}$ are element-wise inverses of the entries in $\boldsymbol{\Upsilon}$ and $\boldsymbol{\Xi}$. Unlike the more conventional optimization metric that maximizes the product SINRs, i.e., $\Pi_u \Upsilon_u \times \Pi_k \Xi_k$, we use the sum of inverse SINRs with $\mathbf{1}_U^T \boldsymbol{\Upsilon}^{-1}$ and $\mathbf{1}_K^T \boldsymbol{\Xi}^{-1}$. This optimization metric allows us to i) *maximize the SINR of each user and target*; ii) *introduce a fairness-on-average to the ISAC system*, and iii) allows for the development of a mathematically easier optimization problem. Finally, since sensing systems have additional processing gains, e.g., signal integration and pulse compression, we introduce the factor $\lambda_s < 1$ to prioritize the communication system when needed.

B. Gradient Descent

To solve the optimization problem, the gradient descent with projection method is employed with the following update rule

$$\boldsymbol{\chi}^{(i+1)} = \boldsymbol{\chi}^{(i)} + \mu \nabla f(\boldsymbol{\chi}^{(i)})$$

where $\boldsymbol{\chi}^{(i)} = [\gamma_1^{(i)}, \dots, \gamma_U^{(i)}, \eta_1^{(i)}, \dots, \eta_K^{(i)}]^T$ contains all the power allocation terms, μ is the gradient step size, also known as *the learning rate*, and $\nabla f(\boldsymbol{\chi}^{(i)})$ is *the gradient of the objective function* for γ_u and η_k. The power allocations will be updated at each iteration as follows

$$\gamma_u^{(i+1)} = \gamma_u^{(i)} - \mu \frac{\partial f}{\partial \gamma_u}, \quad \eta_k^{(i+1)} = \eta_k^{(i)} - \mu \frac{\partial f}{\partial \eta_k}.$$

To ensure that the total power constraint is satisfied at each step of the gradient descent, *the power allocations are scaled according to the total allocated power* as follows

$$\boldsymbol{\chi}_{proj}^{(i+1)} = \begin{cases} \boldsymbol{\chi}^{(i+1)} & p^{(i+1)} \leq P_T \\ \boldsymbol{\chi}^{(i+1)} \times P_T / p^{(i+1)} & p^{(i+1)} > P_T \end{cases}$$

where $p^{(i+1)} = \mathbf{1}_{K+U}^T \boldsymbol{\chi}^{(i+1)}$ corresponds to the total allocated power at iteration $(i+1)$. Then, the norm of the gradient vector is used as the convergence condition, defined as $\|\nabla f(\gamma_u, \eta_k)\| < \epsilon$ where ϵ is a threshold that determines the convergence. The derivative of the objective function f for a generic variable χ is given as

$$\frac{\partial f}{\partial \chi} = -\left(\mathbf{1}_U^T \boldsymbol{\Upsilon}^{-2} \frac{\partial \boldsymbol{\Upsilon}}{\partial \chi} + \lambda_s \mathbf{1}_K^T \boldsymbol{\Xi}^{-2} \frac{\partial \boldsymbol{\Xi}}{\partial \chi} \right) \tag{7}$$

where χ is either γ_u or η_k. The derivatives of the SINR terms are given as

$$\begin{aligned} \frac{\partial \Upsilon_u}{\partial \gamma_u} &= \frac{\alpha_u}{\mathcal{D}_\Upsilon}, \; \frac{\partial \Upsilon_u}{\partial \eta_k} = -\frac{\gamma_u \alpha_u \alpha_{u,k}}{\mathcal{D}_\Upsilon^2} \\ \frac{\partial \Xi_k}{\partial \eta_k} &= \frac{\beta_k}{\mathcal{D}_\Xi}, \; \frac{\partial \Xi_k}{\partial \gamma_u} = -\frac{\eta_k \beta_k \beta_{k,u}}{\mathcal{D}_\Xi^2} \end{aligned}$$

where $\mathcal{D}_\Upsilon$ and $\mathcal{D}_\Xi$ correspond to the denominators of SINR terms given in (3) and (5), respectively. By obtaining these closed-form expressions, the computational complexity of the optimization problem is significantly reduced.

IV. Numerical Analysis

In this section, numerical analyses demonstrate our proposed approach. The users are simulated with random channel coefficients following a Rayleigh distribution, while the targets are simulated with deterministic paths for LoS and Rayleigh-distributed coefficients for multipath. The total available power $P_T = 1$ Watt is equally distributed among 100 active subcarriers, giving $P_{T_q} = 0.01$ Watts per subcarrier. In all cases, the initial power allocation is uniform among the users and targets, i.e., $\gamma_u = \eta_k = P_T/(K+U), \forall k, u$. We assume that the user and target SINRs are obtained from the channel-sounding session and a prior sensing session, respectively. Assuming that 64 pulses will be used for range/Doppler processing, we prioritize the communication subsystem by setting $\lambda_s = 1/64$, the learning rate is $\mu = 10^{-6}$, and $N_T = 8$.

A. Single Realization of ISAC Power Allocation

In Fig. 1, a single realization is depicted. At each iteration, the power allocation is updated using gradient descent, and the corresponding SINRs are computed across all subcarriers based on (3) and (5).

First of all, the allocated powers are consistently lower for the targets compared to the users, reflecting the prioritization of the communication subsystem. The initial SINRs for the users are 12 dB and 3 dB, while the targets start at 14 dB and 9 dB. Over 80 iterations, the power allocations are adjusted to (a) boost user SINRs by 6 dB and 11 dB, which will significantly improve the bit-error rate, and (b) decrease target SINRs by approximately 12 dB, which will be compensated for by radar processing gain[3].

[3]The radar processing gain in OFDM systems ranges from 30 to 50 dB [14], which is sufficient enough to improve target detection accuracy in this configuration.

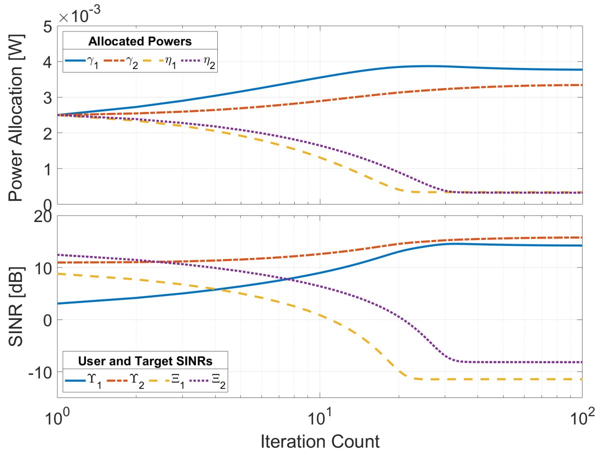

Fig. 1: Gradient descent solution for two users and two targets. The SINRs are derived based on the allocated powers.

B. SINR Distributions Before and After ISAC Power Allocation

In Fig. 2, the overall performance of ISAC power allocation is evaluated across ten thousand channel realizations. For each realization, the initial SINRs (before optimization, BO) are computed, the optimization problem is solved, and the final SINRs (after optimization, AO) are obtained. The cumulative probability of initial and final SINRs are shown for each user and target, accompanied by their mean and standard deviation.

From the communication perspective, the user SINRs improve by approximately 8 dB on average and concentrate around the mean SINR, while the standard deviation reduces by 5 dB. These enhancements will significantly improve the bit-error rate[4] and ensure stable communication quality. From the sensing perspective, the average target SINRs decrease by approximately 12 dB, which will be compensated by radar processing gain as shown by the black line. The target SINRs also exhibit better concentration around the mean value, supporting reliable and consistent target detection. Regarding the whole ISAC system after optimization, the user and target SINRs are balanced on average within each subsystem (but not necessarily per realization) and the SINR discrepancy is much lower, showing the benefit of using the sum of inverse SINRs in the objective function.

C. Mean and Standard Deviation of SINR Distributions

In Fig. 3, the numerical analysis focuses on the mean and standard deviation of SINR distributions as the number of sensing targets K and the communication users U vary. In all cases, increasing K or U reveals a gradual decrease in the average SINR of users and targets. This is expected since all users and targets share the total available power. Hence, their signal power decreases, affecting the interference power on other users/targets. However, the effect of reduced signal power is more pronounced. Furthermore, a significant decrease in the standard deviation after optimization is present in all variations, as well as the improved mean SINR of users and purposefully reduced mean SINR of targets. Finally, since users experience lower path loss compared to the targets, the overall SINR distribution of the communication subsystem is slightly higher than the one of the sensing subsystem.

[4]For comparison, 64-QAM modulation at 5 dB and 15 dB yields roughly 10^{-1} and 10^{-5} bit-error rate, respectively.

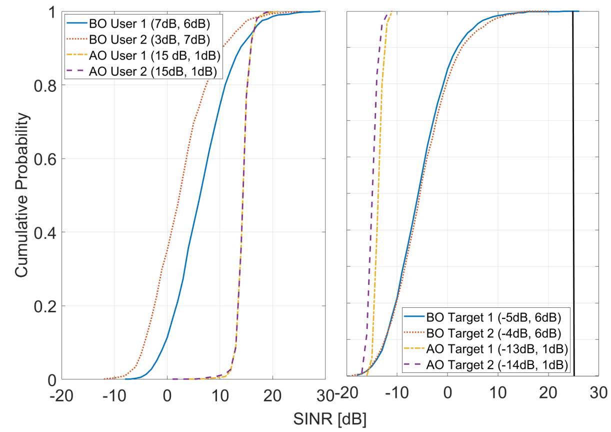

Fig. 2: The impact of the proposed ISAC power allocation on overall user and target SINR distributions. The number pairs in the legends correspond to (the mean, the standard deviation) of each SINR distribution. The black line shows the targets' SINR once the radar processing gain is applied as $10\log_{10}(100 \times 64)$.

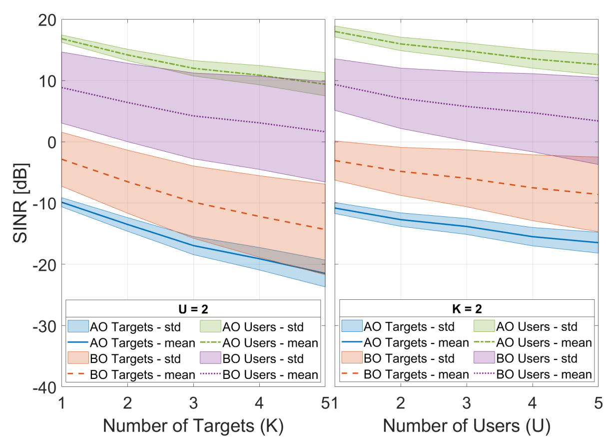

Fig. 3: Figure on the left: $U = 2$ and K ranges from 1 to 5. Figure on the right: $K = 2$, and U ranges from 1 to 5.

V. Conclusion

We proposed a novel approach to enable ISAC in WLAN systems that requires minimal upgrades. By adapting the existing MU-MIMO precoder scheme for simultaneous communication and sensing, and decoupling power allocation from beamforming, the proposed framework significantly reduces implementation complexity while ensuring compatibility with the existing WLAN standards. A flexible optimization framework is introduced to balance SINR across communication users and sensing targets. Numerical results demonstrate the ability of our approach to achieve balanced SINR and enhance overall ISAC performance under various configurations. Future work should focus on more complex scenarios as well as analytical and experimental performance evaluations.

References

[1] O. Bejarano, E. W. Knightly, and M. Park, "IEEE 802.11 ac: From Channelization to Multi-user MIMO," *IEEE Communications Magazine*, vol. 51, no. 10, pp. 84–90, 2013.

[2] R. Du, H. Hua, H. Xie, X. Song, Z. Lyu, M. Hu, Y. Xin, S. McCann, M. Montemurro, T. X. Han *et al.*, "An Overview on IEEE 802.11 bf: WLAN Sensing," *IEEE Communications Surveys & Tutorials*, 2024.

[3] Y. Ma, G. Zhou, and S. Wang, "WiFi Sensing with Channel State Information: A Survey," *ACM Computing Surveys (CSUR)*, vol. 52, no. 3, pp. 1–36, 2019.

[4] J. A. Zhang, F. Liu, C. Masouros, R. W. Heath, Z. Feng, L. Zheng, and A. Petropulu, "An Overview of Signal Processing Techniques for Joint Communication and Radar Sensing," *IEEE Journal of Selected Topics in Signal Processing*, vol. 15, no. 6, pp. 1295–1315, 2021.

[5] F. Liu, L. Zhou, C. Masouros, A. Li, W. Luo, and A. Petropulu, "Toward Dual-functional Radar-communication Systems: Optimal Waveform Design," *IEEE Transactions on Signal Processing*, vol. 66, no. 16, pp. 4264–4279, 2018.

[6] F. Liu, C. Masouros, A. Li, H. Sun, and L. Hanzo, "MU-MIMO Communications with MIMO Radar: From Co-existence to Joint Transmission," *IEEE Transactions on Wireless Communications*, vol. 17, no. 4, pp. 2755–2770, 2018.

[7] X. Liu, T. Huang, N. Shlezinger, Y. Liu, J. Zhou, and Y. C. Eldar, "Joint Transmit Beamforming for Multiuser MIMO Communications and MIMO Radar," *IEEE Transactions on Signal Processing*, vol. 68, pp. 3929–3944, 2020.

[8] F. Liu, Y. Xiong, K. Wan, T. X. Han, and G. Caire, "Deterministic-random tradeoff of integrated sensing and communications in gaussian channels: A rate-distortion perspective," in *2023 IEEE International Symposium on Information Theory (ISIT)*. IEEE, 2023, pp. 2326–2331.

[9] H. Hua, J. Xu, and T. X. Han, "Optimal Transmit Beamforming for Integrated Sensing and Communication," *IEEE Transactions on Vehicular Technology*, vol. 72, no. 8, pp. 10 588–10 603, 2023.

[10] J. Johnston, L. Venturino, E. Grossi, M. Lops, and X. Wang, "MIMO OFDM Dual-function Radar-communication under Error Rate and Beampattern Constraints," *IEEE Journal on Selected Areas in Communications*, vol. 40, no. 6, pp. 1951–1964, 2022.

[11] O. Alp Topal, Ö. Tuğfe Demir, E. Björnson, and C. Cavdar, "Multi-Target Integrated Sensing and Communications in massive MIMO Systems," *arXiv e-prints*, pp. arXiv–2410, 2024.

[12] A. R. Chiriyath, B. Paul, G. M. Jacyna, and D. W. Bliss, "Inner Bounds on Performance of Radar and Communications Co-existence," *IEEE Transactions on Signal Processing*, vol. 64, no. 2, pp. 464–474, 2016.

[13] A. R. Chiriyath, B. Paul, and D. W. Bliss, "Radar-Communications Convergence: Coexistence, Cooperation, and Co-design," *IEEE Transactions on Cognitive Communications and Networking*, vol. 3, no. 1, pp. 1–12, 2017.

[14] W. Zhou, R. Zhang, G. Chen, and W. Wu, "Integrated Sensing and Communication Waveform Design: A Survey," *IEEE Open Journal of the Communications Society*, vol. 3, pp. 1930–1949, 2022.

[15] H. C. Yildirim, L. Storrer, J. Louveaux, P. De Doncker, and F. Horlin, "Impact of MU-MIMO on Passive Wi-Fi Sensing: Threat or Opportunity?" in *2022 2nd IEEE International Symposium on Joint Communications Sensing (JCS)*, 2022, pp. 1–6.

[16] H. C. Yildirim, L. Storrer, M. Willame, J. Louveaux, P. De Doncker, and F. Horlin, "Passive Wi-Fi-based Radars with 802.11ax MU-MIMO Signals: AoD Estimation with A Single Antenna," in *2023 IEEE 3rd International Symposium on Joint Communications Sensing (JCS)*, 2023, pp. 1–6.

[17] H. C. Yildirim, L. Storrer, M. Willame, J. Louveaux, and F. Horlin, "Enabling MIMO Radars in WLAN Sensing: From Spatial Multiplexing to Beamsteering," in *2024 21st European Radar Conference (EuRAD)*, 2024, pp. 67–70.

[18] C. Ravelo, D. Martín-Sacristán, and J. F. Monserrat, "Exploiting Zero Forcing and Block Diagonalization Precoding for Multi-User MIMO ISAC: Bridging Communications and Sensing," *IEEE Access*, 2024.

[19] J. P. González-Coma, J. Rodríguez-Fernández, N. González-Prelcic, L. Castedo, and R. W. Heath, "Channel Estimation and Hybrid Precoding for Frequency Selective Multiuser mmWave MIMO Systems," *IEEE Journal of Selected Topics in Signal Processing*, vol. 12, no. 2, pp. 353–367, 2018.

[20] J. Liu, Z. Luo, and X. Xiong, "Low-Resolution ADCs for Wireless Communication: A Comprehensive Survey," *IEEE Access*, vol. 7, pp. 91 291–91 324, 2019.

[21] R. Zhang, L. Cheng, S. Wang, Y. Lou, Y. Gao, W. Wu, and D. W. K. Ng, "Integrated Sensing and Communication with Massive MIMO: A Unified Tensor Approach for Channel and Target Parameter Estimation," *IEEE Transactions on Wireless Communications*, 2024.

[22] G. D. Durgin, *Space-Time Wireless Channels*. Prentice Hall Professional, 2003.